# Dynamics of Six Generations of PAMAM Dendrimers As Studied by Dielectric Relaxation Spectroscopy

**Jovan Mijović,*,† Sanja Ristić,† and Jose Kenny‡**

*Othmer-Jacobs Department of Chemical and Biological Engineering, Polytechnic University, Six Metrotech Center, Brooklyn, New York 11201, and Department of Materials Science and Technology, University of Perugia, 05100 Terni, Italy*

*Received March 14, 2007; Revised Manuscript Received May 8, 2007*

ABSTRACT: Broadband dielectric relaxation spectroscopy (DRS) was employed to study molecular dynamics of the first six generations of poly(amidoamine) (PAMAM) dendrimers with ethylenediamine core and amino surface groups. DRS was performed over a wide range of frequency and temperature. Dendrimers show distinctly different relaxation behavior below and above the temperature of −30 °C, which roughly corresponds to their calorimetric $T_g$. Three relaxation processes are observed below −30 °C, and an explanation of their molecular origin is provided. The interplay between molecular architecture and hydrogen bonding was found to have an effect on dielectric relaxation that is not found for dynamic mechanical relaxation. All those processes are characterized by Arrhenius-like temperature dependence. Above −30 °C, the spectra are dominated by conductivity and are analyzed using the dielectric modulus and conductivity formalisms. The average relaxation time for the segmental process was calculated from the dielectric loss modulus spectra and found to be of the Vogel−Fulcher−Tammann (VFT) type. An additional process, termed "conductivity relaxation", was observed in the modulus spectra under certain conditions, and an explanation of its molecular origin is offered.

## Introduction

Dendrimers, also known as cauliflower or starburst polymers, are nanoscopic globular macromolecules whose architecture consists of three domains: (1) *core*, which can be a single atom or a group of atoms, (2) *branch units*, which divide radially grown concentric layers termed generations, and (3) *functional surface groups*, which play a key role in determining the properties.[1] The first cascade synthesis of what is today referred to as dendrons was performed by Vogtle et al.,[2] while the first dendrimers synthesis was described by Denkewalter et al.[3] in a U.S. patent. The first published papers on dendrimers were by Newkome et al.[4] and Tomalia et al.[5] They used a route named divergent growth, in which the dendrimer was synthesized in a stepwise manner from a central core. One advantage of this method is the possibility of modifying the dendrimer surface by altering the end groups in the outermost generation, so that the overall chemical and physical properties of the dendrimer can be tailored to specific needs. An alternative method, named convergent growth, in which synthesis starts at the periphery and is propagated toward the core, was developed by Fréchet.[6] The pioneering studies on dendrimers were focused mainly on the development of synthetic routes, and as a result, a large number of dendrimers with variety of architectures have been prepared, as described in several texts.[7,8]

But despite a considerable amount of research on dendrimers, only a few reports have been published about their dynamics. Of experimental techniques available for the study of dynamics, dielectric relaxation spectroscopy (DRS) is rapidly becoming a dominant tool.[9,10] The great attraction of DRS derives from an unparalleled frequency window (up to 16 decades) that enables one to probe molecular dynamics of condensed matter over a broad range of time scales and length scales that may not be available by other spectroscopic, scattering, and relaxation methods. DRS has been employed to study phosphorus-containing dendrimers[11−13] and carbosilane dendrimers with perfluorinated[14] and cyanobiphenyl[15] end groups. One common finding in those studies is that dendrimers exhibit typical relaxation characteristics of glass-forming materials. Interestingly, however, there have been no reports of DRS studies of poly(amidoamine) (PAMAM) dendrimers. These materials continue to generate considerable interest among scientists, most recently as promising candidates for efficient DNA delivery systems.[16] PAMAM dendrimers have been investigated by dynamic mechanical spectroscopy (DMS),[17] but that study was limited to a narrow frequency range and the temperature range between 15 and 105 °C above their glass transition temperature.

By studying dynamics on the nanoscopic and microscopic level, we learn important information about the physics that underlies processing, structure, and properties on the macroscopic level. A number of fundamental questions about the origin, the time scale, and the length scale of various molecular motions in dendrimers remain unresolved. Thus, the principal objective of this study is to conduct a systematic investigation of a series of PAMAM dendrimers and quantify the effect of molecular and external factors on their dynamics. To the best of our knowledge, this study marks the first published report on the dynamics of PAMAM dendrimers as studied by DRS.

## Experimental Section

Generations 0−5 of poly(amidoamine) (PAMAM) dendrimers with ethylenediamine core and amino surface groups were obtained from Aldrich. Dendrimers were supplied in methanol solution (generations 0, 1, 2, and 3 at 20 wt %, generation 4 at 10 wt %, and generation 5 at 5 wt %). The model compound, *N*-(2-aminoethyl)acetamide, was also obtained from Aldrich. The molecular structures of *N*-(2-aminoethyl)acetamide and the first three dendrimer generations are presented in Figure 1. The glass transition

* To whom correspondence should be addressed. E-mail: jmijovic@poly.edu.
† Polytechnic University.
‡ University of Perugia.

10.1021/ma070624q CCC: $37.00 
Published on Web 06/15/2007

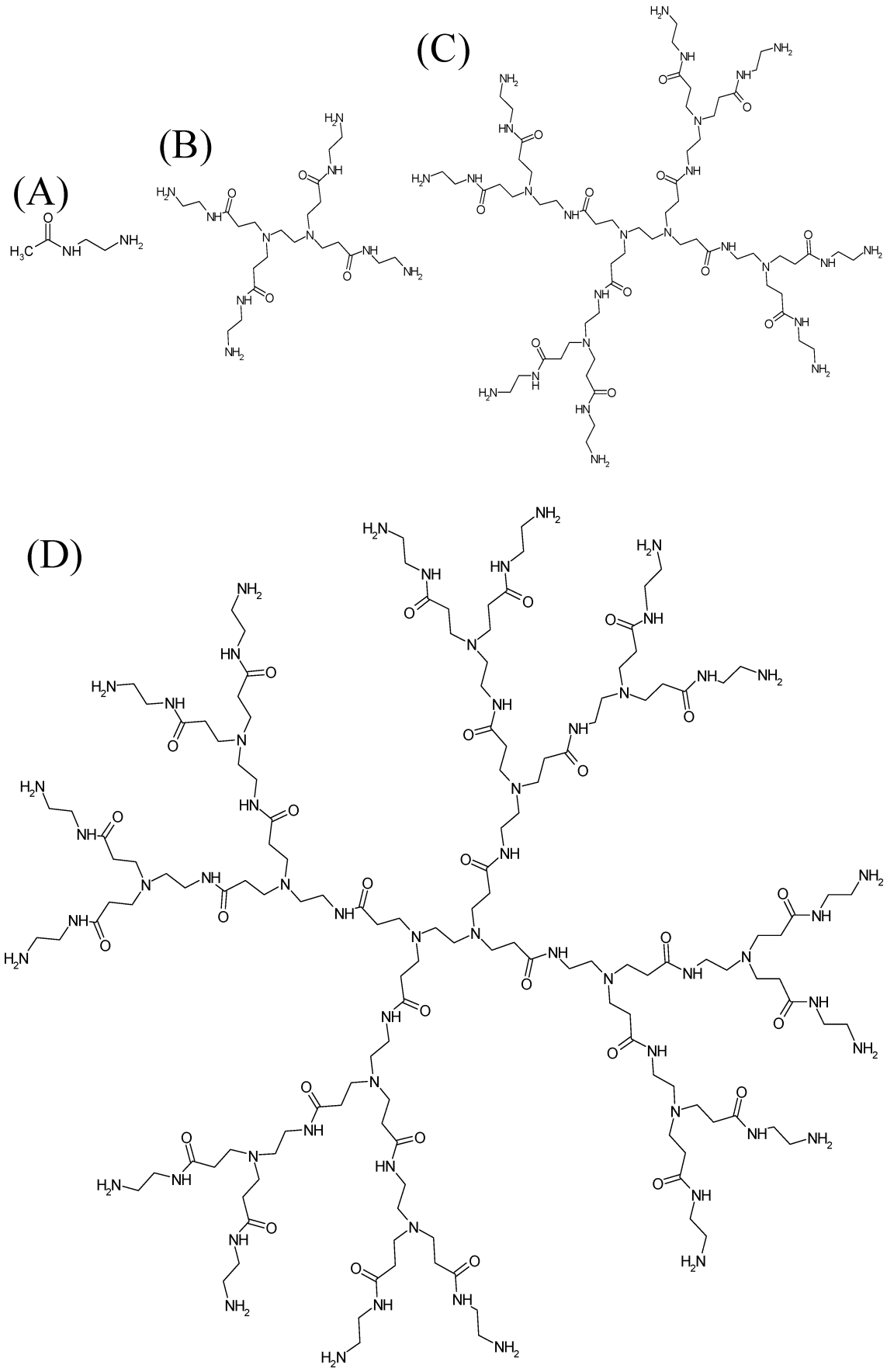


**Figure 1.** Molecular structure of *N*-(2-aminoethyl)acetamide (A) and PAMAM dendrimers generation 0 (B), generation 1 (C), and generation 2 (D).

temperature was determined by differential scanning calorimetry (DSC) using a TA Instruments Co. DSC model 2920. Samples were first cooled to −50 °C and then heated at 10 °C/min to 50 °C. Samples for dielectric measurements were placed in a dielectric

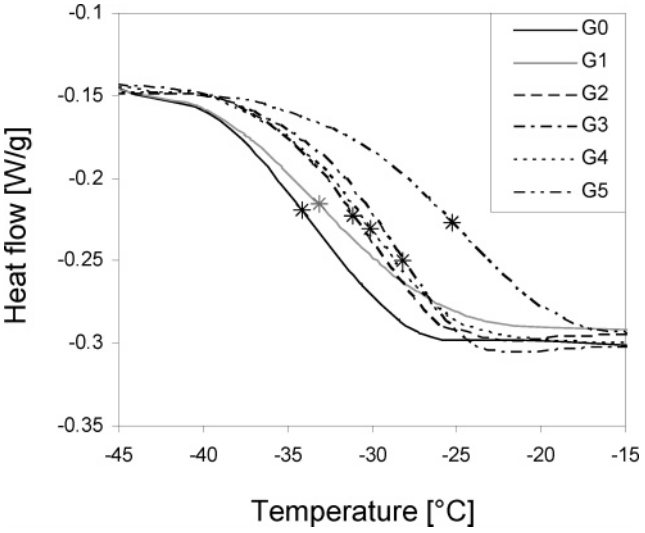


**Figure 2.** DSC plot for six generations of PAMAM dendrimers.

**Table 1. Number of Surface Groups ($Z$), Molecular Weight ($M_w$), and Glass Transition Temperatures ($T_g$) of First Six Generations of PAMAM Dendrimers**

| generation | $Z$ | $M_w$ | $T_g$ (°C) |
|---|---|---|---|
| 0 | 4 | 517 | −34 |
| 1 | 8 | 1430 | −33 |
| 2 | 16 | 3256 | −31 |
| 3 | 32 | 6909 | −28 |
| 4 | 64 | 14215 | −30 |
| 5 | 128 | 28826 | −25 |

cell and kept in a vacuum oven at 60 °C for 7 days in order to remove the solvent completely. PAMAM dendrimers are in the liquid state at room temperature and thermally stable below 120 °C.[17] Samples were placed between two aluminum electrodes, 12 mm in diameter and with 50 $\mu$m spacing between them. All dielectric measurements were performed in the frequency range from $10^{-2}$ to $10^{8}$ Hz using two different experimental setups. In the range from $10^{-2}$ to $10^{6}$ Hz measurements were made with Novocontrol α analyzer and from $10^{6}$ to $10^{8}$ Hz with Hewlett-Packard 4291B RF impedance analyzer. Both instruments are interfaced to computers via IEEE 488.2 and are connected to a heating/cooling unit (modified Novocontrol Novocool System), which can control temperature from −100 to 250 °C with a precision of ±0.5 °C. Isothermal dielectric spectra were generated in the temperature range from −100 to 100 °C. Further details about our experimental facility for dielectric measurements are given elsewhere.[18,19]

## Results and Discussion

**Differential Scanning Calorimetry (DSC).** The sole thermal transition observed in all six generations of dendrimers was the glass transition ($T_g$). The $T_g$ was calculated from the midpoint of the heating trace in the transition range for each sample, indicated by a star in Figure 2, and the results are listed in Table 1. The $T_g$ varies between −25 and −34 °C and is a weak increasing function of generation number.

**Dielectric Relaxation Spectroscopy (DRS).** DRS study was conducted in the temperature range from −100 to 100 °C. Dynamics of dendrimers were significantly different below and above −30 °C, and for that reason our results will be presented and discussed separately for the temperature range from (1) −100 to −30 °C and (2) −20 to 100 °C. The temperature ranges below −30 °C and above −20 °C correspond roughly to the regions above and below the DSC $T_g$, respectively.

*1. Dynamics in the Temperature Range from −100 to −30 °C.* Dynamics below the DSC $T_g$ are examined first: this is the region where no segmental motions occur. Figure 3 shows dielectric loss in the frequency domain for the model compound (Figure 3A) and for the following PAMAM dendrimers: generation 0 (Figure 3B), generation 1 (Figure 3C), generation 2 (Figure 3D), generation 3 (Figure 3E), generation 4 (Figure 3F), and generation 5 (Figure 3G). Below −30 °C all dendrimers are characterized by three relaxation processes, termed $\beta$, $\gamma$, and $\delta$ in the order of increasing frequency at constant temperature. The location of each process is indicated by an arrow in each figure. The $\gamma$ process in generations 0 and 3 is present but is hidden in the frequency range between the $\beta$ and $\delta$ processes. As seen in Figure 3A, the dielectric behavior of the model compound is dominated by conductivity even at very low temperature. Therefore, only the $\delta$ process (the fastest process) can be described with certainty in the model compound.

Dielectric spectra of dendrimers were fitted to a summation of three Havriliak−Negami (HN) functions[20] and a conductivity term. For the model compound we used two HN functions and the conductivity contribution. The equation used relates the complex permittivity to the frequency of the alternating electromagnetic field according to

$$\epsilon^*(\omega) = \epsilon' - i\epsilon'' = -i\left(\frac{\sigma_c}{\epsilon_0\omega}\right)^N + \sum_{k=1}^{3}\left[\frac{\Delta\epsilon_k}{(1+(i\omega\tau_k)^{a_k})^{b_k}} + \epsilon_{\infty k}\right] \quad (1)$$

where $\epsilon_0$ is the vacuum permittivity, $\sigma_c$ is the conductivity, $a$ and $b$ are the shape parameters of the HN equation that define the breadth and the symmetry of the spectrum, respectively, and $\tau$ is the average relaxation time.

The Havriliak−Negami function reduces to the Debye equation when $a = b = 1$, the Cole−Cole equation[21] when $b = 1$, and the Cole−Davidson equation[22] when $a = 1$. All processes observed in this study in dendrimers and in the model compound were symmetric at all temperatures, thus reducing the fitting function to a superposition of three Cole−Cole equations plus the conductivity term, resulting in

$$\epsilon^*(\omega) = \epsilon' - i\epsilon'' = -i\left(\frac{\sigma_c}{\epsilon_0\omega}\right)^N + \sum_{k=1}^{3}\left[\frac{\Delta\epsilon_k}{1+(i\omega\tau_k)^{a_k}} + \epsilon_{\infty k}\right] \quad (2)$$

Deconvolution of the spectra reveals the characteristics of each relaxation process. The time scales and the length scales of these processes reflect the molecular architecture of specific parts of dendrimers and their interactions with the oscillating electromagnetic field during measurement. In what follows we shall build our discussion of relaxation dynamics in dendrimers around the effect of their architecture on the frequency location for the maximum loss, the temperature dependence of the average relaxation time, the dielectric relaxation strength, and the shape of the relaxation spectra. Finally, we shall describe the molecular origin of each relaxation.

We begin by examining the $\beta$ process in all dendrimers. The lowest frequency process, termed the $\beta$ process, shows a typical behavior of the well-known Johari−Goldstein $\beta$ process, common to glass formers. The loss peak shifts to higher frequency and increases in intensity with increasing temperature. Dielectric relaxation strength of the $\beta$ process increases with temperature, as shown in Figure 4A. An anomalous result was observed for generation 3, and we shall revert to this finding later in the text. Figure 5 shows the average relaxation time as a function of temperature for the $\beta$ process in all six generations. The

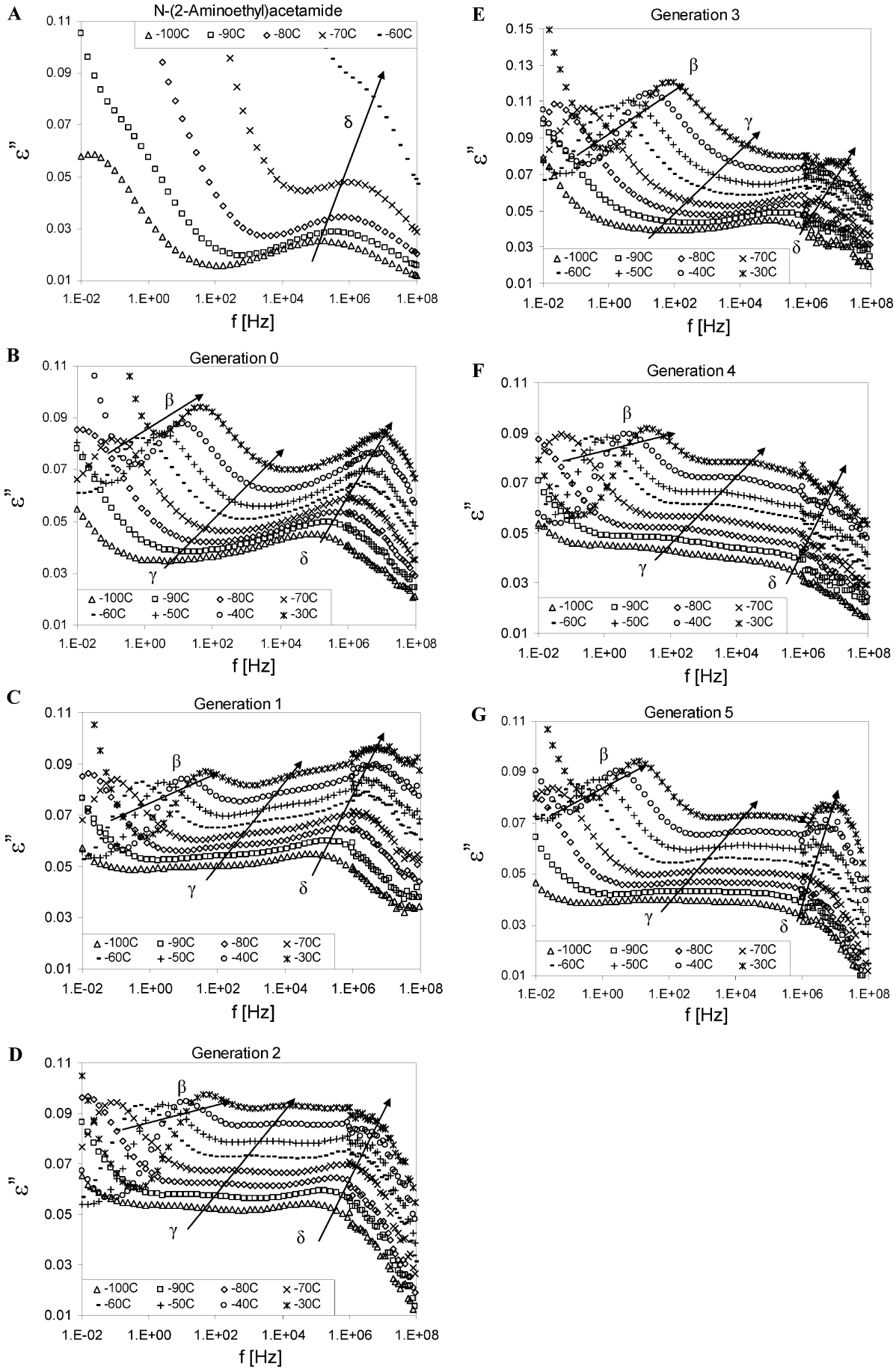


**Figure 3.** Dielectric loss in the frequency domain with temperature as a parameter for (A) model compound, (B) generation 0, (C) generation 1, (D) generation 2, (E) generation 3, (F) generation 4, and (G) generation 5.

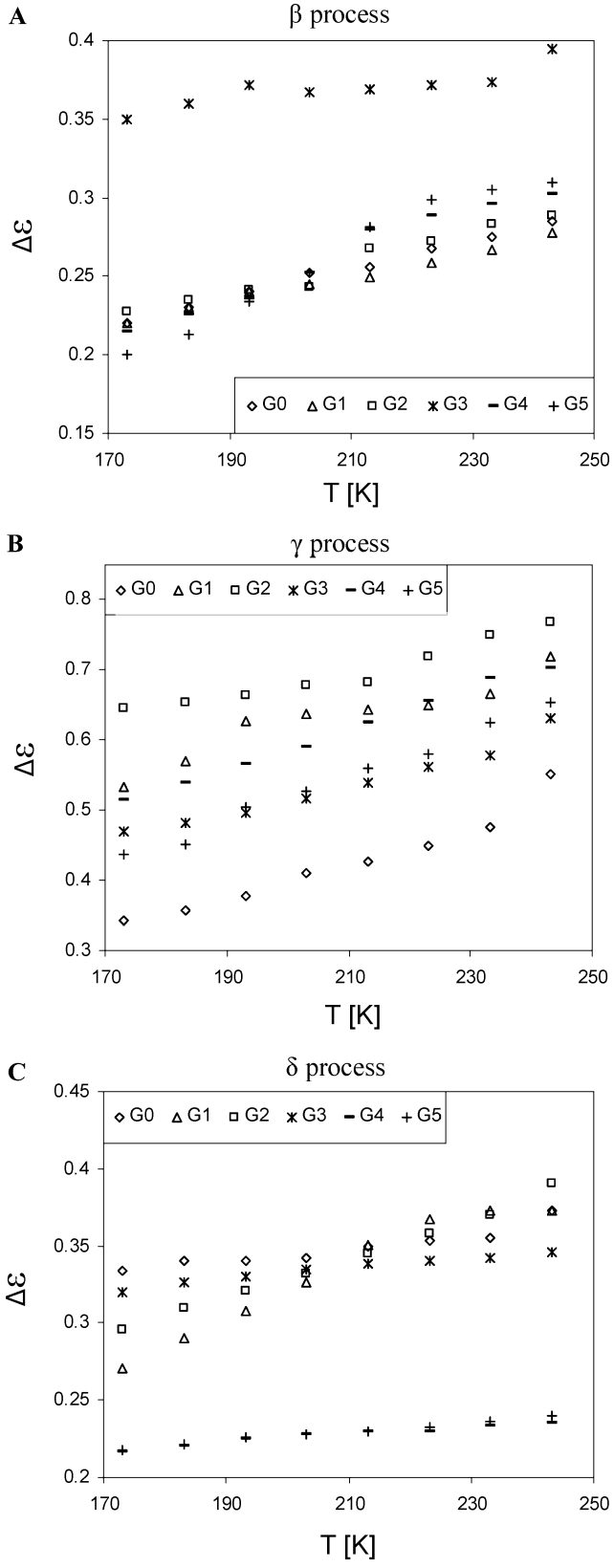


**Figure 4.** Dielectric relaxation strength as a function of temperature with generation number as a parameter for (A) $\beta$ process, (B) $\gamma$ process, and (C) $\delta$ process.

relationship between the average relaxation time and temperature is Arrhenius-like and can be described by

$$\tau = \tau_0 \exp\left(\frac{E_a}{RT}\right) \tag{3}$$

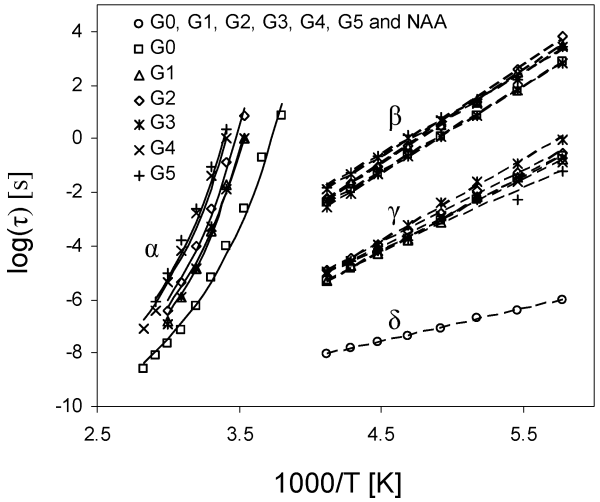


**Figure 5.** Average relaxation time as a function of reciprocal temperature for all processes in dendrimers and the model compound.

**Table 2. Activation Energies for Local Processes**

| | $E_a$ (kJ/mol) | | |
|---|---|---|---|
| generation | $\beta$ | $\gamma$ | $\delta$ |
| 0 | 60.2 | 54.8 | 23.4 |
| 1 | 66.1 | 53.6 | 23.4 |
| 2 | 69.4 | 51.0 | 23.4 |
| 3 | 61.5 | 58.2 | 23.4 |
| 4 | 59.4 | 48.5 | 23.4 |
| 5 | 59.0 | 43.5 | 23.4 |

where $E_a$ is the activation energy and $\tau_0$ is a proportionality constant. The calculated values of the activation energy were 60.2 kJ/mol for generation 0, 66.1 kJ/mol for generation 1, 69.4 kJ/mol for generation 2, 61.5 kJ/mol for generation 3, 59.4 kJ/mol for generation 4, and 59.0 kJ/mol for generation 5. The calculated values of activation energy for each process are summarized in Table 2. The HN parameter $a$ for the $\beta$ process, which describes the spectrum breadth, does not vary with generation number but decreases with increasing temperature from 0.50 to 0.43.

The $\gamma$ process is examined next. The loss peak also shifts to higher frequency, and its intensity increases with increasing temperature. Figure 4B depicts dielectric relaxation strength as a function of temperature for this process. No apparent trend as a function of generation number is observed, and an explanation for this behavior is offered below. The temperature dependence of the average relaxation time follows the Arrhenius equation for all generations, as seen in Figure 5. The activation energy for the $\gamma$ process varies as follows: 54.8 kJ/mol for generation 0, 53.6 kJ/mol for generation 1, 51.0 kJ/mol for generation 2, 58.2 kJ/mol for generation 3, 48.5 kJ/mol for generation 4, and 43.5 kJ/mol for generation 5. Note that the activation energy for this process decreases with increasing molecular weight, with the exception of generation 3. The $\gamma$ process is very broad but thermodielectrically simple. The HN breadth parameter $a$ is independent of temperature and is constant at 0.2 for all six generations.

Finally we look at the $\delta$ process. The frequency location of the maximum loss for the $\delta$ process at a given temperature is identical for all six generations and is consistent with the high-frequency process in the model compound. The peak intensity and the frequency at maximum loss increase with increasing temperature, and the HN parameter $a$ increases slightly from 0.28 to 0.36. Dielectric relaxation strength of this process, plotted as a function of temperature in Figure 4C, increases with

increasing temperature for all dendrimers. However, it is interesting to note that the relaxation strength for generations 4 and 5 appears to be out of sequence with respect to other generations. The temperature dependence of the average relaxation time follows the Arrhenius form, as shown in Figure 5, with the calculated activation energy of 23.4 kJ/mol common to all dendrimers and the model compound.

We now focus attention on the molecular origin of sub-$T_g$ relaxations, starting with the $\delta$ process. This is the fastest (highest frequency) process that is present in all generations and in the model compound and has the common origin in motions of terminal amino groups on the outer surface of dendrimers. This interpretation is in agreement with the DRS study of phosphorus-containing dendrimers[12] and hyperbranched polyglycerol,[23] where the fastest relaxation was assigned to the local motions of terminal groups. The $\delta$ process is very broad in the frequency domain because these groups find themselves in a variety of local environments, each with its local barrier to reorientation.

The molecular origin of the $\gamma$ process lies in the motions of amide groups that are not involved in hydrogen bonding. The dielectric strength of the $\gamma$ process is determined by the interplay between the dendrimer architecture and intra- and intermolecular hydrogen bonding according to the following scenario. Generation 0 dendrimers are open molecules with short branches and large spaces between them, as shown in Figure 1B. Ample interpenetration occurs between different molecules, and hence intermolecular hydrogen bonding is dominant. Intramolecular hydrogen bonding is negligible. Generations 1 and 2 are also open, domelike molecules,[17] and their architecture, shown in Figure 1C,D, remains conducive to the penetration of arms of one dendrimer between those of others and the formation of intermolecular hydrogen bonds between the amide groups on different molecules. But while intermolecular hydrogen bonding remains the dominant mechanism, its intensity decreases with increasing generation number from 0 to 1 to 2. The architecture of generation 3 dendrimers becomes increasingly complex and less amenable to the interpenetration between dendrimers, leading to a notable decrease in intermolecular and an increase in intramolecular hydrogen bonding. Generation 4 dendrimers are said to be fully developed,[24,25] and the likelihood of intermolecular hydrogen bonding decreases even further. At the same time, however, there is a continuing increase (from generation 3 to 5) in intramolecular hydrogen bonds that involve amide groups on different branches of the same dendrimer.

The following experimental evidence offers support for the proposed molecular origin of $\gamma$ *r*elaxation. The dielectric strength for the $\gamma$ process increases with increasing generation number from 0 to 2 (see Figure 4B). This is a direct consequence of the decrease in intermolecular hydrogen bonding with increasing generation number that results in a higher concentration of non-hydrogen-bonded amide groups. The interplay between vanishing intermolecular and emerging intramolecular hydrogen bonding in generations 3 and 4 leads to a decrease followed by an increase in the strength of the $\gamma$ process. Generation 5 is dominated by intramolecular hydrogen bonding that is further enhanced by back-folding of the end groups,[26] and the engagement of additional amide groups results in the decrease in dielectric strength. Our results also demonstrate that dielectric relaxation spectroscopy is sensitive to molecular architecture in a way not encountered in dynamic mechanical relaxation.

Finally, we identify the origin of the $\beta$ process in dendrimers. On the basis of the similarity in the chemical structure of the model compound and the branch end segments in dendrimers, and the observation that the slower (lower frequency) relaxation in the model compound (at a frequency of about $10^{-2}$ Hz at $-100$ °C) appears in the frequency range of the $\beta$ process, we assign this process to the local fluctuations of branch ends which include amino groups. This is additionally supported by the results of a study of ester-terminated, amide-based dendrimers,[27] where a possible mechanism for $\beta$ relaxation was proposed involving molecular motions of dipolar segments that include $-NH_2$ end groups. The $\beta$ process is broad because the individual local reorientations occur with different rates in different local environments.

*2. Dynamics in the Temperature Range from −20 to 100 °C.* This is the region above the calorimetric $T_g$ of dendrimers, where one expects to detect the segmental process. However, dielectric permittivity and loss are masked by strong conductivity in this temperature range, necessitating an alternative strategy for the identification of relaxation processes. The most informative formalism for the presentation of dielectric spectra for ionically conducting system is a matter of debate. In this study we employ two distinct methodologies to investigate the DRS spectra at temperatures above −20 °C: (1) the dielectric modulus formalism[27−32] and (2) the conductivity representation.[31−34]

*2.1. Dielectric Modulus Formalism* In highly charged materials, such as polyelectrolytes and ionic glasses and melts, the dielectric modulus is often the preferred form of data presentation. Our data are expressed in terms of dielectric modulus, $M^*$, which is defined as the inverse of complex permittivity, $\epsilon^*$, where $\epsilon^* = \epsilon' - i\epsilon$ and $M^* = M' + i' M''$ such that

$$M' + iM'' = (\epsilon' - i\epsilon'')^{-1} \tag{4}$$

resulting in

$$M' = \frac{\epsilon'}{(\epsilon')^2 + (\epsilon'')^2} \quad \text{and} \quad M'' = \frac{\epsilon''}{(\epsilon')^2 + (\epsilon'')^2} \tag{5}$$

The modulus and the permittivity formalisms contain information from the same measurement, but they differ in the manner in which the underlying dielectric phenomena are suppressed or highlighted.[31] For instance, $\epsilon''(f)$ spectra suppress low-frequency relaxation that is often pronounced in $M''(f)$ plots. For generation 0 this behavior is illustrated in Figure 6, which shows the loss component of dielectric permittivity and modulus in the frequency domain, for temperatures below and above the DSC $T_g$ (Figure 6, A and B, respectively). The result for temperatures below $T_g$ is included in this section for the sake of completion. It is seen in Figure 6A that the sub-$T_g$ $\beta$ process is well pronounced in both permittivity (solid lines) and modulus (dash lines) representation, though the loss modulus spectra are slightly broader and are shifted to higher frequency. On the other hand, at temperature above $T_g$ (Figure 6B), the process corresponding to segmental relaxation is hidden in the permittivity representation (solid lines) but is visible in the modulus representation (dashed lines).

For the Debye process a direct correlation between the locations of maximum loss in the two formalisms is given by[32]

$$\tau_M = \frac{\epsilon_\infty}{\epsilon_S}\tau_\epsilon \tag{6}$$

where $\epsilon_\infty$ and $\epsilon_S$ represent real permittivity in the limit of high and low frequency, respectively. In Figure 7, we plot the average relaxation time for the $\beta$ process in generation 0 obtained from the two formalisms as a function of reciprocal temperature.

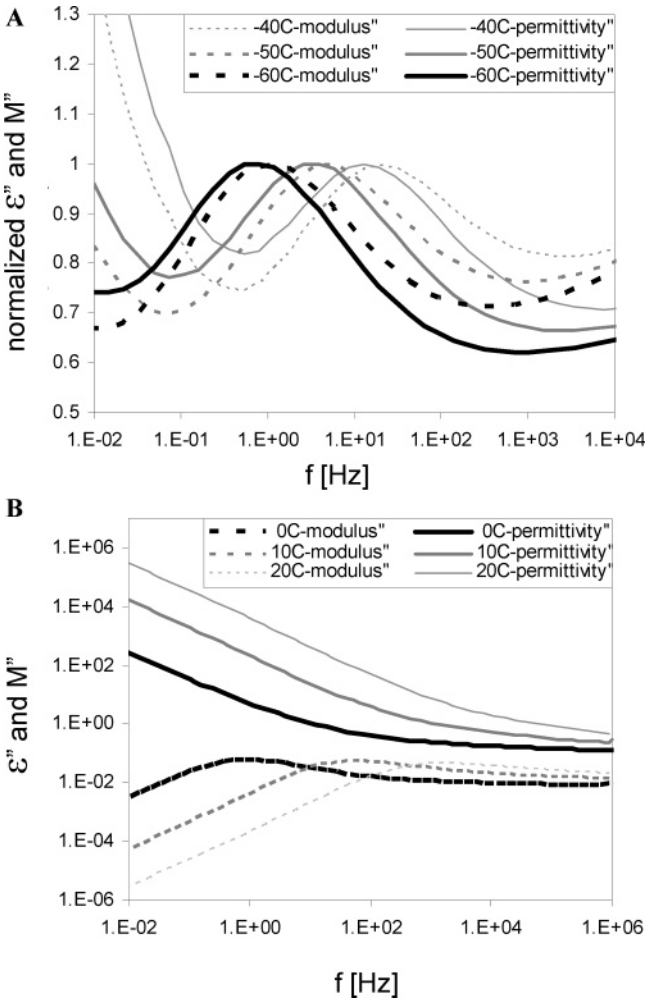


**Figure 6.** Loss component of dielectric permittivity and modulus in the frequency domain for generation 0 for an arbitrary relaxation: (A) below $T_g$ and (B) above $T_g$.

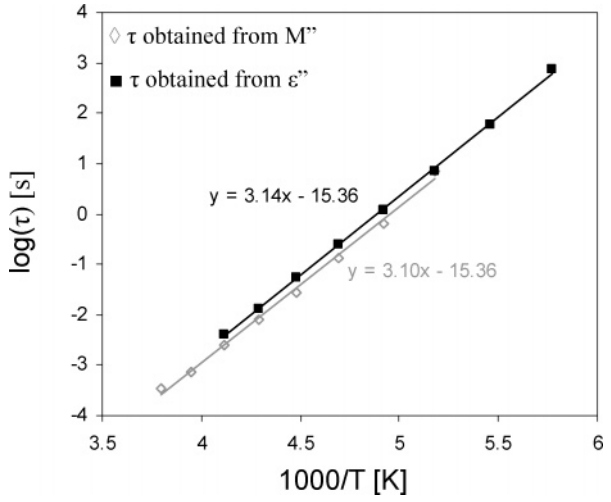


**Figure 7.** Relaxation time as a function of reciprocal temperature for the $\beta$ process in generation 0 obtained from permittivity and modulus formalisms.

Excellent agreement is apparent, and the two plots yield the same activation energy. In the remainder of the text we use the modulus formalism to analyze data above −30 °C, and while acknowledging that $\tau_M$ and $\tau_\epsilon$ are not identical, we refer to the value obtained from the maximum in the dielectric loss modulus as the average relaxation time.

The effect of temperature on the imaginary part of the dielectric modulus in the frequency domain for generations 0 through 5 is presented in Figure 8A−F. A process is readily identified in the loss modulus spectra of all dendrimers, and we refer to it as the α process. This process mimics α relaxation in glass formers as it shifts to higher frequency and decreases in intensity with increasing temperature. The decrease in the peak intensity persists up to about 40 °C for generations 0, 1, and 3 (Figure 8, A, B, and D), 50 °C for generation 2 (Figure 8C), and 60 °C for generations 4 and 5 (Figure 8, E and F). Above these temperatures, the α process merges with the $\beta$ process and the intensity of the combined $\alpha\beta$ relaxation increases. The dielectric modulus spectra of several polymers exhibit, in addition to the α and $\beta$ processes, an additional process termed "conductivity relaxation".[27,33,34] Segmental and conductivity relaxations have similar time scales and hence often overlap.[34] In dendrimers, these two processes are indistinguishable at lower temperatures. However, as temperature approaches 80 °C in generation 0, 70 °C in generation 1, and 60 °C in generations 2 and 3, the first signs of conductivity relaxation become visible. This is demonstrated in Figure 9, which shows dielectric loss modulus in the frequency domain with temperature as a variable for generation 2. Conductivity relaxation appears as a small shoulder at 60 °C and becomes more pronounced with increasing temperature (see arrow). The peak at higher frequency in the modulus spectra of Figure 9 is due to the above-mentioned $\alpha\beta$ process. We note that "conductivity relaxation" is not visible as a separate process in generations 4 and 5. The reason for this behavior can be traced to the dominant role of two different types of hydrogen bonds in lower (than 3) and higher (than 4) generations. As previously discussed, in generations 0 through 3, hydrogen bonding occurs predominantly between amide groups on two different molecules, forming a network with a more uniform morphology, which restricts the mobility of ions. In generations 4 and 5, intermolecular hydrogen bonding is replaced with intramolecular hydrogen bonding. This facilitates the motion of ions through the space between dendrimers and results in the observed decrease in the time scale of conductivity relaxation.

The average relaxation time for the α process, obtained from the frequency of maximum loss modulus, as a function of inverse temperature is presented in Figure 5. The temperature dependence of the relaxation time for the α process in glass formers (see, e.g., Kremer and Schonhals[35]) cannot be parametrized by the Arrhenius law and is commonly described by the Vogel−Fulcher−Tammann (VFT) equation:

$$\tau = \tau_0 \exp\left(\frac{B}{T - T_V}\right) \tag{7}$$

where $\tau_0$ refers to attempt frequency and has the value of $10^{-14}$ s and $T_V$ is the Vogel temperature, which is usually 30−70 K below $T_g$. Empirically, it has been observed that the time scale of glass transition is of the order of 100−1000 s, which corresponds to $10^{-2}$−$10^{-3}$ Hz.

The solid lines that depict the α process in Figure 5 are VFT fits, and we note a very good agreement between the data and the results of regression analysis. The VFT temperature dependence for the α process in dendrimers has also been observed for ester-terminated amide-based dendrimers[27] and carbosilane dendrimers with perfluorinated end groups.[14] The VFT parameters for all six generations are summarized in Table 3. In addition, this table contains the values of dielectric glass transition defined as the temperature where $f_{max}$ equals $10^{-2}$ Hz.

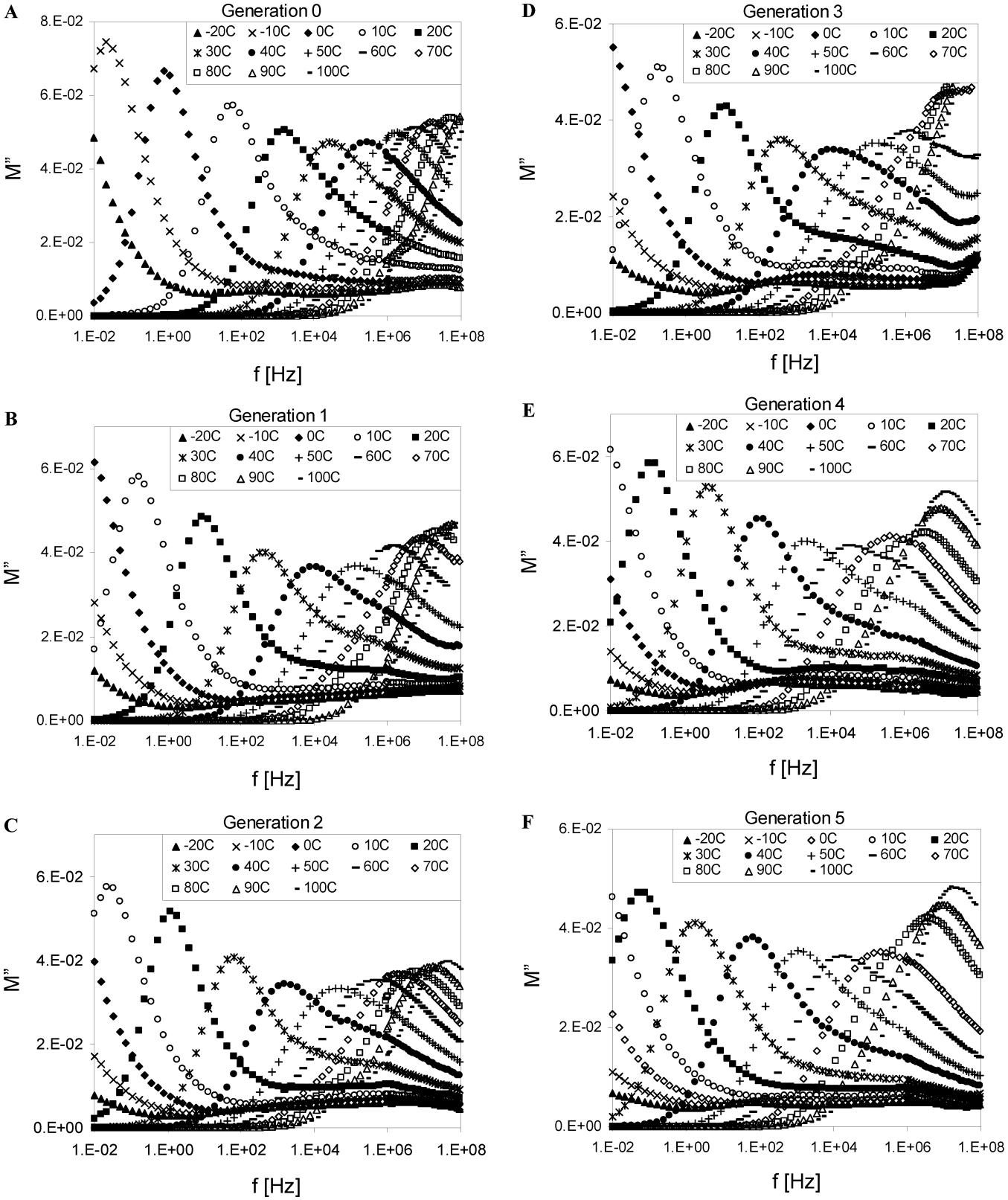


**Figure 8.** Dielectric loss modulus in the frequency domain for generation 0 (A), 1 (B), 2 (C), 3 (D), 4 (E), and 5 (F) in the temperature range from −20 to 100 °C.

*2.2. Conductivity Representation* The second method employed to analyze the data entails the use of conductivity spectra. Ionic conductivity, $\sigma$, is defined by the following relationship:[33]

$$\sigma = \epsilon'' \omega \epsilon_0 \tag{8}$$

where $\omega$ is the angular frequency ($2\pi f$) and $\epsilon_0$ is the permittivity of free space ($8.85 \times 10^{-12}$ F/m). At low frequencies, $\sigma(\omega)$ is constant at the dc value. At higher frequencies the conductivity increases according to a power law, where $\sigma(\omega) \sim \omega^p$ ($0 < p \leq 1$). Figure 10A represents conductivity in the frequency domain with temperature as a parameter for generation 0. The

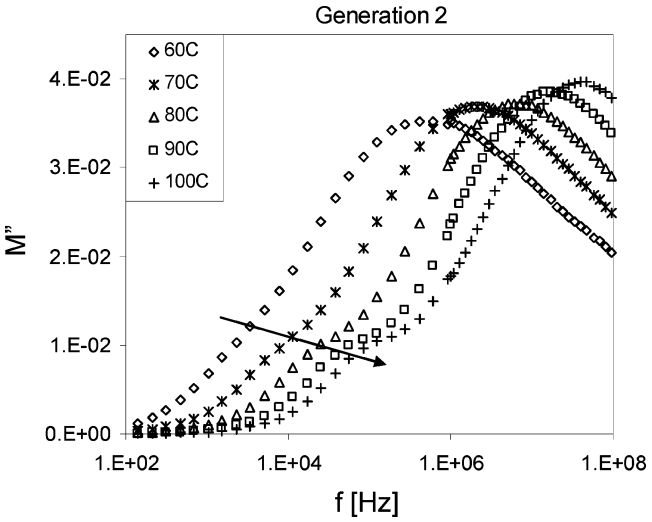


**Figure 9.** Dielectric loss modulus in the frequency domain with temperature as a parameter for generation 2.

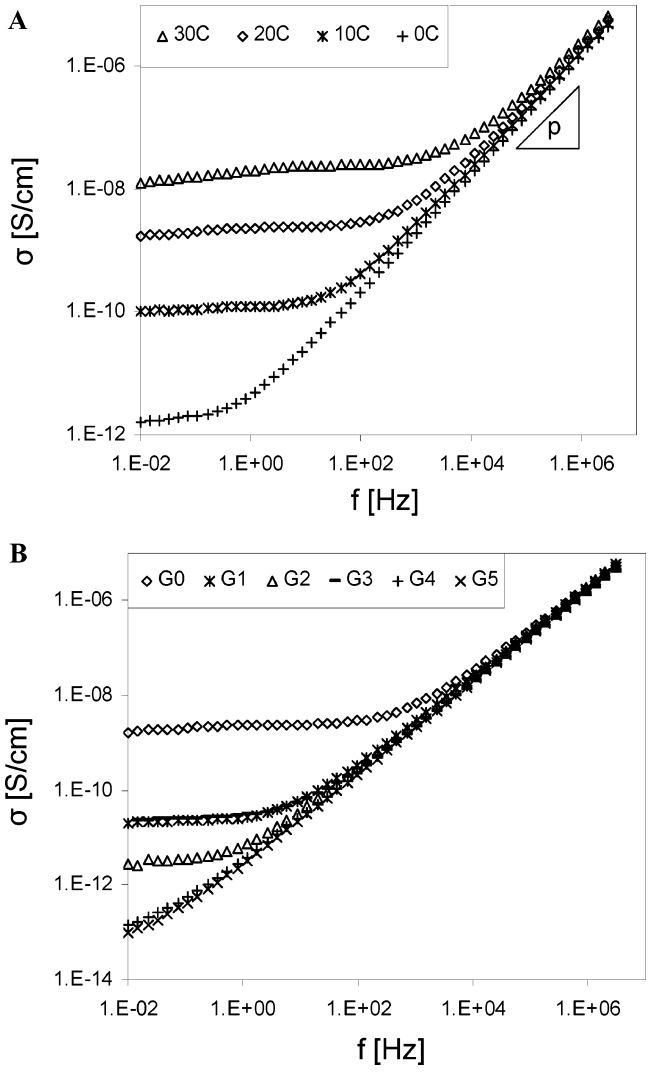


**Figure 10.** Conductivity in the frequency domain with (A) temperature as a parameter for generation 0 and (B) generation number as a parameter.

dc conductivity increases with increasing temperature in this and other generations. Figure 10B shows conductivity vs frequency with generation number as parameter at 20 °C. It is evident that dc conductivity is highest in generation 0 and lowest in generation 5.

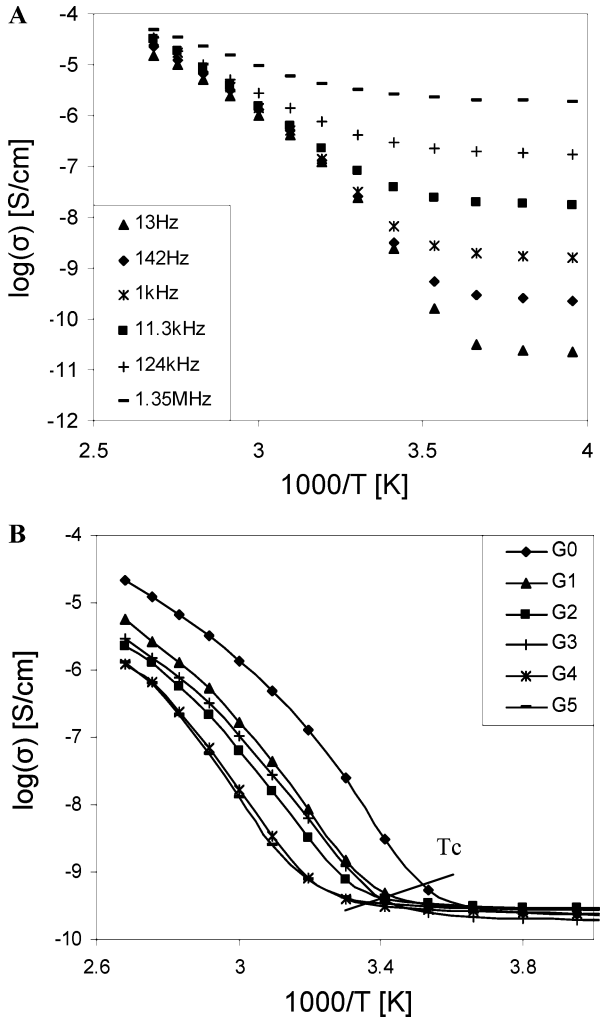


**Figure 11.** Conductivity vs reciprocal temperatures with (A) frequency as a parameter for generation 0 and (B) generation number as a parameter at 142 Hz.

**Table 3. VFT Parameters for Segmental Process**

| generation | $\tau_0$ | $B$ (K) | $T_V$ (K) | $T_g^{Diel}$ (K) |
|---|---|---|---|---|
| 0 | $1.0 \times 10^{-14}$ | 1646 | 220 | 267 |
| 1 | $1.0 \times 10^{-14}$ | 1778 | 227 | 278 |
| 2 | $1.0 \times 10^{-14}$ | 1934 | 228 | 283 |
| 3 | $1.0 \times 10^{-14}$ | 1970 | 222 | 278 |
| 4 | $1.0 \times 10^{-14}$ | 2066 | 229 | 288 |
| 5 | $1.0 \times 10^{-14}$ | 2084 | 230 | 290 |

An alternative way of presenting and analyzing our data is displayed in Figure 11, where conductivity is plotted as a function of reciprocal temperature with frequency as a parameter for generation 0 (Figure 11A) and with generation number as a parameter at constant frequency of 142 Hz (Figure 11B). At lower temperatures, where dielectric relaxation is dominant, the conductivity is strongly dependent on frequency, as seen in Figure 11A. The frequency dependence of conductivity decreases with increasing temperature and practically vanishes at 100 °C (the highest measured temperature). A non-Arrhenius temperature dependence of conductivity is observed for all six generations above some threshold temperature, indicated as $T_c$ in Figure 11B. Below $T_c$, conductivity is constant and independent of the generation number. We acknowledge that Starkweather and Avakian[33] reported a linear relationship between the logarithm of conductivity and reciprocal temperature for several linear polyamides. They pointed out, however, that their data covered a narrow temperature range, making

it difficult to distinguish between the Arrhenius and the VFT behavior.

## Conclusions

We have completed an investigation of the dynamics of first six generations (0 through 5) of PAMAM dendrimers by dielectric relaxation spectroscopy (DRS). Experimental results were generated over the frequency range from $10^{-2}$ to $10^{8}$ Hz and at temperatures from −100 to +100 °C. The dynamics of dendrimers were significantly different below and above their calorimetric $T_g$ located around −30 °C.

Three relaxation processes were observed below −30 °C in all generations and were termed $\beta$, $\gamma$, and $\delta$ in the order of increasing frequency at constant temperature. All three processes are characterized by symmetric, Cole−Cole type relaxation spectra and an Arrhenius-like temperature dependence of the average relaxation time. Moreover, they shift to higher frequency and increase in intensity with increasing temperature. The origin of each process was established by comparing the dielectric response of dendrimers and a low molecular weight model compound. The $\beta$ process is assigned to the local fluctuations of branch ends which include amino groups. The $\gamma$ process was affected by the interplay between molecular architecture and hydrogen bonding. This process is attributed to the motions of the amide groups that are not hydrogen bonded to the neighboring chains. The origin of the $\delta$ process lies in the motions of amino groups on the surface of dendrimers.

In the temperature range from −20 to 100 °C, the spectra were dominated by conductivity and were analyzed using the dielectric modulus formalism and conductivity representation. All dendrimers are characterized by a pronounced dielectric modulus peak which shifts to higher frequency and decreases in intensity with increasing temperature. This process has the characteristics of α relaxation in glass formers and is referred to as such. With increasing temperature the α process merges with the $\beta$ process, giving rise to the combined $\alpha\beta$ relaxation. Conductivity relaxation first appears as a small shoulder in generations 0−3. In generations 4 and 5, however, conductivity relaxation has a shorter time scale and is indistinguishable from segmental relaxation. This behavior is caused by the difference in the architecture (topology) of lower and higher generations. The temperature dependence of the average relaxation time for the α process is of the Vogel−Fulcher−Tammann type.

Low-frequency ionic conductivity is constant at the dc value. At higher frequencies the conductivity increases with frequency according to a power law: $\sigma(\omega) \sim \omega^p$ $(0 < p \leq 1)$. The frequency dependence of conductivity decreases with increasing temperature and practically vanishes at 100 °C (the highest measured temperature). Conductivity decreases with increasing generation number and shows a non-Arrhenius temperature dependence above a threshold value for all six generations.

**Acknowledgment.** This material is based on work supported by National Science Foundation under Grant DMR-0346435. We are grateful to Dr. Dejan Zecevic of Yale University for helpful discussion of the nonlinear and spatially inhomogeneous dendrimer dynamics.

## References and Notes

(1) Caminade, A. M.; Laurent, R.; Majoral, J. P. *Adv. Drug Delivery Rev.* **2005**, *57*, 2130.
(2) Buhleier, E.; Wehner, W.; Vogtle, F. *Synthesis* **1978**, 155.
(3) Denkewalter, R. G.; Kolc, J.; Lukasavage, W. J. US Pat. 4289872, 1981.
(4) Newkome, G. R.; Yao, Z.; Baker, G. R.; Gupta, V. K. *J. Org. Chem.* **1985**, *50*, 2003.
(5) Tomalia, D. A.; Baker, H.; Dewald, J.; Hall, M.; Kallos, G.; Martin, S.; Roeck, J.; Smith, P. P. *Polym. J.* **1985**, *17*, 117.
(6) Hawker, C. J.; Fréchet, J. M. J. *J. Am. Chem. Soc.* **1990**, *112*, 7638.
(7) Newkome, G. R.; Moorefield, C. N.; Vogtle, F. *Dendritic Molecules: Concepts, Syntheses and Perspectives*, VCH: Weinheim, Germany, 1996.
(8) Fréchet, J. M. J.; Tomalia, D. A. *Dendrimers and Other Dendritic Polymers*; Wiley: West Sussex, England, 2001.
(9) Williams, G. Dielectric relaxation spectroscopy of amorphous polymer systems. The modern approach. In *Keynote Lectures in Polymer Science*; Riande, E., Ed.; CSIC: Madrid, 1995.
(10) Riande, E.; Diaz-Calleja, R. *Electrical Properties of Polymers*; Marcel Dekker: New York, 2004.
(11) Dantras, E.; Lacabanne, C.; Caminade, A. M.; Majoral, J. P. *Macromolecules* **2001**, *34*, 3808.
(12) Dantras, E.; Caminade, A. M.; Majoral, J. P.; Lacabanne, C. *J. Phys. D: Appl. Phys.* **2002**, *35*, 5.
(13) Dantras, E.; Dandurand, J.; Lacabanne, C.; Caminade, A. M.; Majoral, J. P. *Macromolecules* **2004**, *37*, 2812.
(14) Trahasch, B.; Stuhn, B.; Frey, H.; Lorenz, K. *Macromolecules* **1999**, *32*, 1962.
(15) Trahasch, B.; Frey, H.; Lorenz, K.; Stuhn, B. *Colloid Polym. Sci.* **1999**, *277*, 1186.
(16) Zhou, J.; Wu, J.; Hafdi, N.; Behr, J. P.; Erbacher, P.; Peng, L. *J. Chem. Commun.* **2006**, 2362.
(17) Uppuluri, S.; Morrison, F. A.; Dvornic, P. R. *Macromolecules* **2000**, *33*, 2551.
(18) Fitz, B.; Andjelic, S.; Mijovic, J. *Macromolecules* **1997**, *30*, 5227.
(19) Mijovic, J.; Duan, Y.; Miura, N.; Monetta, T. *Polym. News* **2001**, *26*, 251.
(20) Havriliak, S. J.; Negami, S. *Polymer* **1967**, *8*, 161.
(21) Cole, R. H.; Cole, K. S. *J. Chem. Phys.* **1942**, *10*, 98.
(22) Davidson, D. W.; Cole, R. H. *J. Chem. Phys.* **1950**, *18*, 1417.
(23) Garcia-Bernabe, A.; Diaz-Calleja, R.; Haag, R. *Macromol. Chem. Phys.* **2006**, *207*, 970.
(24) Uppuluri, S.; Keinath, S. E.; Tomalia, D. A.; Dvornic, P. R. *Macromolecules* **1998**, *31*, 4498.
(25) Uppuluri, S.; Tomalia, D. A.; Dvornic, P. R. *Polym. Mater. Sci. Eng.* **1997**, *77*, 116.
(26) Bosman, A. W.; Janssen, H. M.; Meijer, E. W. *Chem. Rev.* **1999**, *99*, 1665.
(27) Emran, S. K.; Newkome, G. R.; Weis, C. D.; Harmon, J. P. *J. Polym. Sci., Part B: Polym. Phys.* **1999**, *37*, 2025.
(28) Emran, S. K.; Liu, Y.; Newkome, G. R.; Harmon, J. P. *J. Polym. Sci., Part B: Polym. Phys.* **2001**, *39*, 1381.
(29) Moynihan, C. T. *J. Non-Cryst. Solids* **1996**, *203*, 359.
(30) Wagner, H.; Richert, R. *Polymer* **1997**, *38*, 2.
(31) Sun, M.; Pejanovic, S.; Mijovic, J. *Macromolecules* **2005**, *38*, 985.
(32) Richert, R.; Wagner, H. *Solid State Ionics* **1998**, *105*, 167.
(33) Starkweather, H. W.; Avakian, P. *J. Polym. Sci., Part B: Polym. Phys.* **1992**, *30*, 637.
(34) Shilov, V. V.; Shevchenko, V. V.; Pissis, P.; Kyrtsis, A.; Georgoussis, G.; Gomza, Y. P.; Nesin, S. D.; Klimenko, N. S. *J. Non-Cryst. Solids* **2000**, *275*, 116.
(35) Kremer, F., Schönhals, A., Eds. *Broadband Dielectric Spectroscopy*; Springer-Verlag: Berlin, 2002.

MA070624Q